

Section 5

Development of and studies with regional and smaller-scale atmospheric models, regional ensemble, monthly and seasonal forecasting

Mesoscale ensemble prediction system using the nonhydrostatic atmospheric model COSMO-RU

D. Yu. Alferov (dalferov@mecom.ru), G. S. Rivin (Gdaly.Rivin@mecom.ru)
Hydrometcenter of Russia, Moscow, Russia

Ensemble description

The nonhydrostatic mesoscale atmospheric model COSMO-RU [4, 5] is a version of the COSMO model [3] for European territory of Russia.

In recent years, technological progress has made the mesoscale ensemble weather forecasting possible. Systems for mesoscale ensemble weather prediction already work in United States, Canada and some European countries. Mesoscale ensemble forecasting using COSMO model has become one of the COSMO consortium Perspective Projects [1, 2].

We use the COSMO-RU model with 14 km grid step. The model grid for this version has 350×310 grid points at 40 vertical levels.

Successful experiments on building ensembles by perturbing COSMO mesoscale model physical parameterizations are already made in Italy, Greece and Switzerland [1]. The difference of this work is the use of different numerical schemes implemented in the model too.

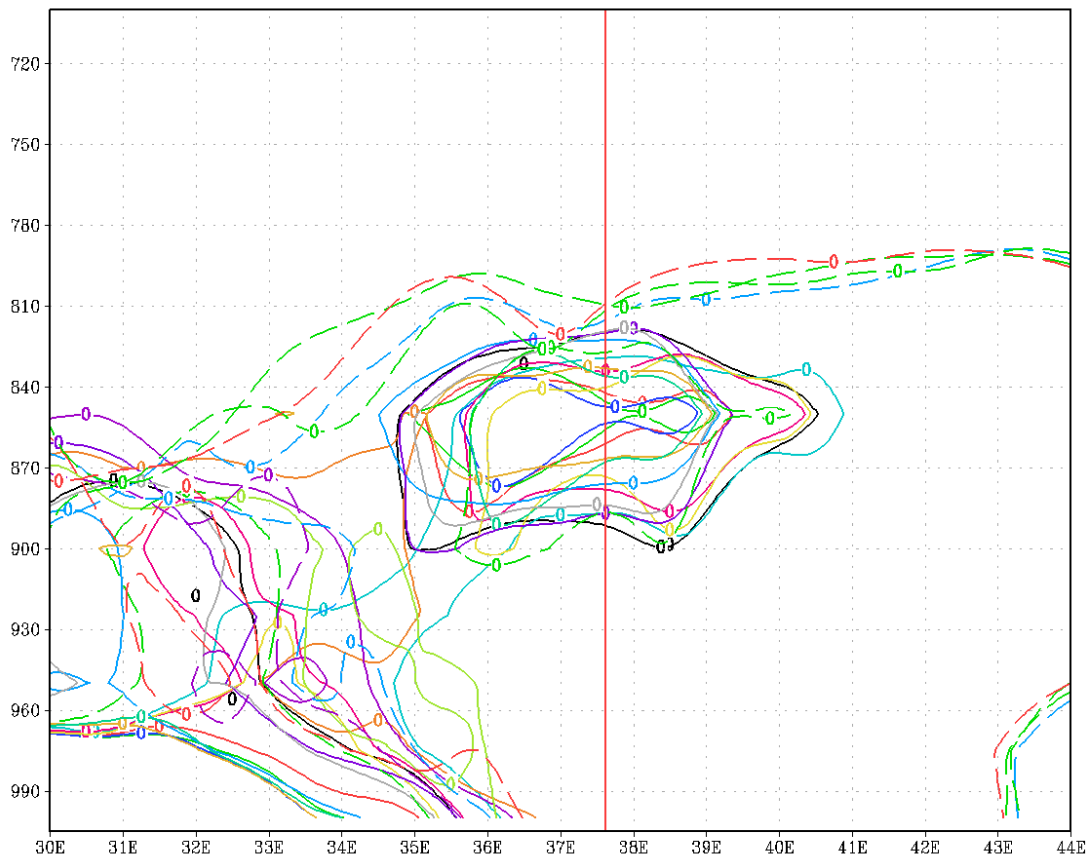
Freezing rain case in Moscow, 25–26 December 2010

Intensive freezing rain in Moscow region on 25-26 December 2010 caused damage of trees, electric lines and constructions due to large mass of glazing ice formed during this time. This case is interesting for ensemble forecast test because of usually low predictability of such phenomena.

The ensemble used in this study contains 28 ensemble members using the leapfrog and 2 different second-order Runge-Kutta numerical schemes, Tiedtke and Kain-Fritsch convection parameterization schemes and perturbations of parameters for the length scale of sub-scale surface thermal patterns over land and the scaling factor for the thickness of the laminar boundary layer for heat.

Fig. 1 shows the 0°C isotherm spaghetti plot on the zonal vertical profile at 6:00 GMT 12/26/2010 according to the 66-hour ensemble forecast. The red vertical line shows the position of Moscow. We can see that even for such a long forecast term our ensemble shows rather large probability for appearance of warm (with temperature greater than 0°C) air flow above the cold near-surface air. This temperature distribution is one of main weather conditions making the freezing rain possible, so it can be an important symptom of freezing rain cases when forecasted.

It should be noted that this ensemble forecast also shows rather large probability of snow and rain in the region at the moment shown. This allows us to see the possibility of freezing rain at this moment. So we can see that our ensemble can predict such phenomena in near 3 days advance.



GrADS: COLA/IGES

2011-03-25-15:11

Fig. 1. 0°C isotherm spaghetti plot on the zonal vertical profile at 6:00 GMT 12/26/2010 according to the 66-hour ensemble forecast. The vertical coordinate is shown in pressure levels. The red vertical line shows the position of Moscow.

References

1. Marsigli C. COSMO Priority Project “Short Range Ensemble Prediction System” (SREPS): Final Report. // COSMO Technical Report No. 13. — Deutscher Wetterdienst, 2009. — 32 p.
2. Montani A., Cesari D., Marsigli C., Paccagnella T. Seven years of activity in the field of mesoscale ensemble forecasting by the COSMO-LEPS system: main achievements and open challenges. // COSMO Technical Report No. 19. — Deutscher Wetterdienst, 2010. — 28 p.
3. Schaettler U., Doms G., Schraff C. A Description of the Nonhydrostatic Regional COSMO-Model. Part VII: User’s Guide. — Deutscher Wetterdienst, 2009. — 142 p.
4. Vil’fand R. M., Rivin G. S., Rozinkina I. A. Mesoscale weather short-range forecasting at the Hydrometcenter of Russia, on the example of COSMO-RU. // Russian Meteorology and Hydrology, 2010. — Vol. 35, No. 1, pp. 1–9.
5. Vil’fand R. M., Rivin G. S., Rozinkina I. A. COSMO-RU system of nonhydrostatic mesoscale short-range weather forecast of the Hydrometcenter of Russia: The first stage of realization and development. // Russian Meteorology and Hydrology, 2010. — Vol. 35, No. 8, pp. 503–514.

A few improvements brought to the French global and fine-scale models

F. Bouysse, Y. Bouteloup, J-F Mahfouf, F. Taillefer, E. Wattrelot
CNRM-GAME, Météo-France and CNRS, Toulouse, France
Francois.bouysse@meteo.fr

A major upgrade of the NWP system in April 2010 has already been described in the 2010 Blue Book. Additional improvements were made at the end of 2010, a few of which are described here.

The representation of stratiform clouds, shallow convective clouds and associated precipitations is based in Arpege and Aladin models on the prognostic evolution of specific humidity for four classes of hydrometeors: cloud liquid water, cloud solid water, rain and snow. Microphysical processes related to precipitation are described explicitly. Sedimentation is computed with a statistical algorithm suitable for "long" time steps (between 9 and 30 minutes). This parameterization of microphysical processes has been improved to correct some deficiencies identified by forecasters. Non zero sedimentation speed, about several centimeters per second, is now taken into account for the liquid and solid cloud water. This modification decreases the cirrus cloud cover in a realistic way and the high sensitivity of the parameterization to the autoconversion threshold for the solid water phase. This change allows a revision of the snow fall speed (0.6 m/s to 1.5 m/s) and of the autoconversion thresholds with a slightly positive impact on the simulation of stratocumulus clouds.

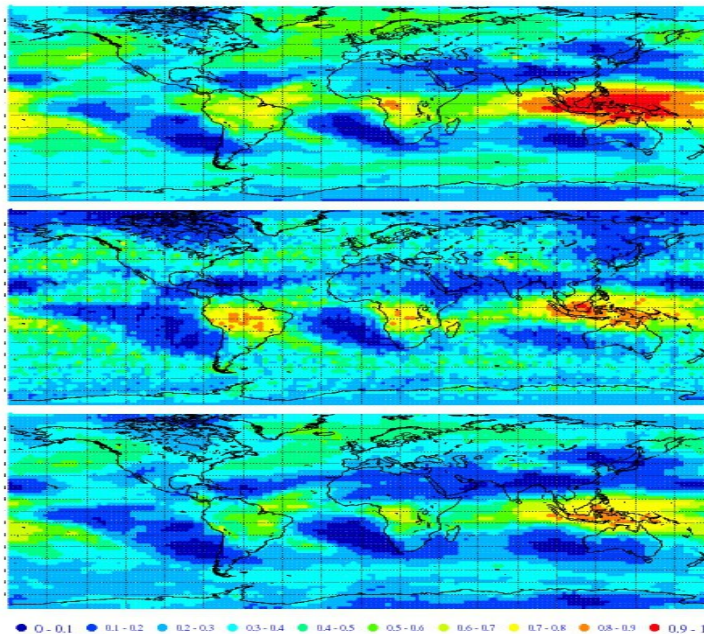


Figure 1: high cloud cover simulated by the ARPEGE model averaged over December-January-February 2007/2008 with the old (top panel) and then new (lower panel) version of microphysics compared to the high cloud cover derived from CALIPSO lidar observations (middle panel).

The numerical weather prediction model AROME has a dedicated 3D-Var data assimilation system providing analyses every 3 hours. This year, it has been possible to assimilate radar reflectivity data, via a 1D+3D approach (Caumont et al, 2010). As can be seen in figure 2, the assimilation of reflectivities improves precipitation detection scores for short range forecasts while, at the same time, retaining a good level of false alarm rate.

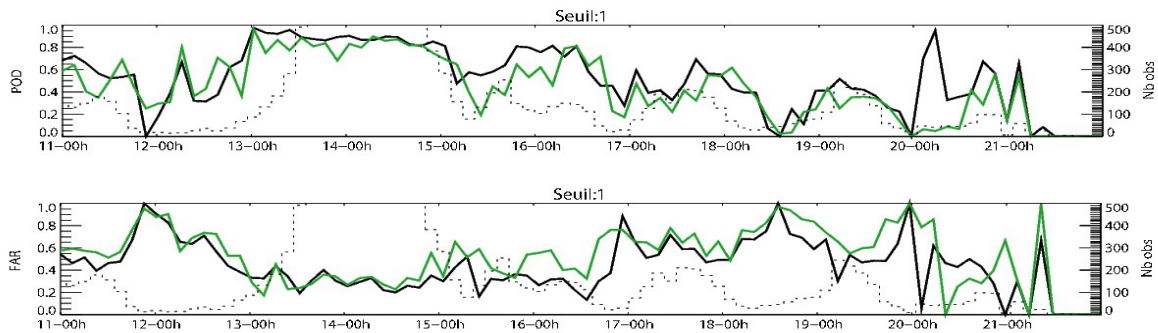


Figure 2: comparison of forecast time-series to rain-gauges On top, probability of detection (POD); bottom, false alarm rate (FAR) for short range cumulated precipitation forecasts between 00h and 03h. Scores show the 1mm/h precipitation threshold for the experiment with the assimilation of radar reflectivities (solid black line), and without the assimilation of radar reflectivities (solid green line), between the 11th and the 21st of December 2008 inclusive. The dashed black line corresponds to the number of observations below the threshold of 1mm/h.

The quality of fine scale forecasts also depends upon the land surface state since it has a strong influence on water and energy exchanges with the atmosphere. In its first operational configuration, the prognostic soil variables of AROME were interpolated from surface analyses produced by the global model ARPEGE. In order for AROME to have its own surface analysis system, a methodology based on the one currently used in the operational models ARPEGE and ALADIN has been set-up. Soil temperature and moisture contents are corrected using screen-level short-range forecasts errors of temperature and relative humidity (Giard and Bazile, 2000). Figure 3 shows that most dry and wet regions are rather consistent over the domain between the two maps. However, the interest of correcting AROME forecasts clearly shows up since small scale features are better resolved particularly over mountainous regions. Quantitative Precipitation Forecasts are systematically improved with the experimental AROME suite.

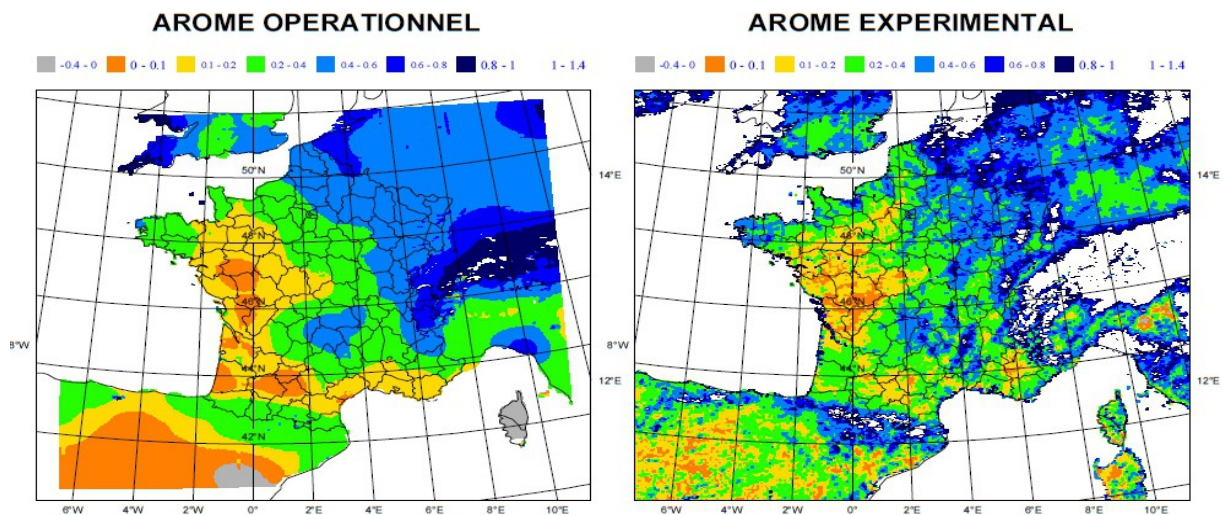


Figure 3: Soil wetness index produced on 1st October 2010 by the operational AROME suite (interpolation from the ARPEGE model) and by an experimental AROME suite (having its own surface analysis)

References:

- Caumont O., V. Ducrocq, E. Wattrelot, G. Jaubert, S. Pradier-Vabre, 2010: 1D+3DVar assimilation of radar reflectivity data: a proof of concept. *Tellus A*, **62A** (2), 173-187, doi: 10.1111/j.1600-0870.2009.00430.x.
- Giard, D., and E. Bazile, 2000: Implementation of a new assimilation scheme for soil and surface variables in a global NWP model. *Mon. Weather Rev.*, **128**, 997-1015

Different Aspects of WRF-ARW applications at the National Meteorological Service – and Naval Hydrographic Service of Argentina.

Estela A Collini^(1,2), Lorena Ferreira⁽¹⁾, Maria E. Dillon^(1,2), Soledad Osoros^(1,2), Gloria Pujol⁽¹⁾, Paula Martin^(2,4), Martina Suaya⁽¹⁾, Arnau Folch⁽³⁾

⁽¹⁾ Servicio Meteorológico Nacional, Argentina; ⁽²⁾ Servicio de Hidrografía Naval, Argentina; ⁽³⁾ Barcelona Supercomputing Centre – Centro Nacional de Supercomputación, Spain; ⁽⁴⁾ Departamento de Ciencias de la Atmósfera y los Océanos, Universidad de Buenos Aires, Argentina.

estela.collini@gmail.com

INTRODUCTION

This is a report of activities of the diverse applications of the numerical weather prediction (NWP) model WRF-ARW implementations developed under a collaborative project between the National Meteorological Service (NMS) and the Naval Hydrographic Service (NHS) of Argentina.

A system composed by WPS, WRF-ARW, ARWpost and WPPV3 is running at the NMS on daily basis for the 00 UTC cycle, on a cluster of 5 ML350 HP Proliant nodes. This version is Open MP and distributed implementation. The model's domain covers South America and the surrounding oceans, with 24 km of spatial resolution and provides 72-hours forecast fields every 3 hs. of precipitation and sea level pressure, maximum CAPE and CIN, RH and TD at 2 m. In addition, 10-meters winds over selected regions of the Argentine coasts and nearby South Atlantic Ocean are produced. Recently, and focused over Argentina, fields such as 700hPa omega and geopotential height, cloud base and 0°C isotherm geopotential height, PBL height and friction velocity, surface visibility, among others, were included for the same cycle. Besides that, there is a broad range of studies underway with the main object of improve the NWP forecasts over the region.

RESEARCH ACTIVITIES

Sensitivity studies of soil moisture initialization

One of the research topics in which we are applying WRF-ARW is to investigate the model sensitivity to the lower boundary condition given by the soil moisture fields, both in its diagnosis as well its short and medium range predictions. To meet this goal, several experiments are carried out by changing the initial soil moisture content.

The impact in the precipitation predictions and over other key variables, are studied using soil moisture data from uncoupled soil global models from the Global Land Data Assimilation System (GLDAS) and the CPTEC (Centro de Previsão de Tempo e Estudos Climáticos) soil model. Normalization procedures to avoid inconsistencies are applied. Preliminary evaluations of the superficial soil moisture fields with passive radiometer AMSR-E, and of the precipitation resulting fields with NMS meteorological stations measurements and CMORPH and TRMM estimations, are in progress. Preliminary results (*Fig. 1*) show the sensitivity of the model to the different lower boundary conditions used, and its influence on the precipitation fields as stated by a number of authors (*Collini et al. 2010, Ferreira et al. 2011*).

Forecast Verification

The validation of weather forecasts consists of comparing the forecast events to the corresponding observed events, in order to establish the quality of the forecast. Different verification attempts focalized on extreme temperatures at the surface and temperature in the whole atmosphere, were made.

Verification of extreme surface temperatures forecasts of the WRF – ARW with the observations from 19 selected Argentine meteorological stations was made on operational basis, following the analysis performed for March, April and May (Southern Hemisphere autumn) of 2010 by *Dillon et al. 2010*, where the basic statistical BIAS and RMSE were utilized. These results were compared with those of the ETA/NMS operational model. Generally, these models showed lower thermal amplitude than the observed. Differences between the models results were mainly due to the parameterizations, since both models use the GFS fields for the initialization and boundary conditions. Additionally, the first stages in the application of Model Evaluation Tool (MET) was carried out to validate temperature forecasted by the model, compared with the 12Z upper air soundings observations from Córdoba, Resistencia and Ezeiza Argentine weather stations (*Martin and Collini, 2010*).

Forecast of ash dispersion and deposition.

With the aim to improve forecasts of volcanic ash dispersion and deposition over Argentina, a number of experiments were made running the FALL3D dispersion model coupled with the WRF-ARW model for the 2008 Chaitén eruption, Chile. The model results include time-dependent 2D and 3D variables like airborne ash

concentration at selected flight levels, cloud column load and deposit thickness among others, and its tracking at selected locations. This work constitutes a preliminary assessment of the application of FALL3D coupled with WRF-ARW at the NMS as a test case, and constitutes a starting point for the application of this modeling strategy to other volcanoes of the region (Folch et al., 2011).

CONCLUSIONS

This project contemplates various numerical modeling issues and, hopefully, its results will be used not only for operational purposes but also as a framework for future developments focused on the Argentine weather and climatic system.

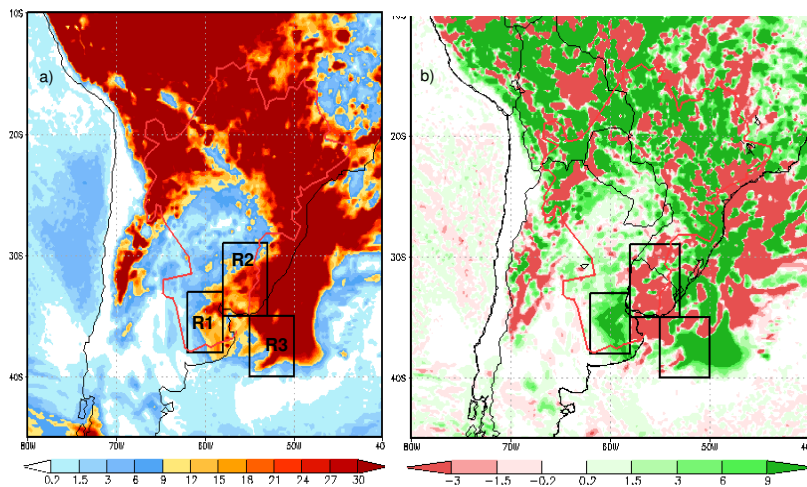


Fig 1. 120 hs accumulated precipitation (mm) forecasted by WRF-CTRL model (left) and its difference respect to WRF-CPTEC model (right). The squares show studied subregions.

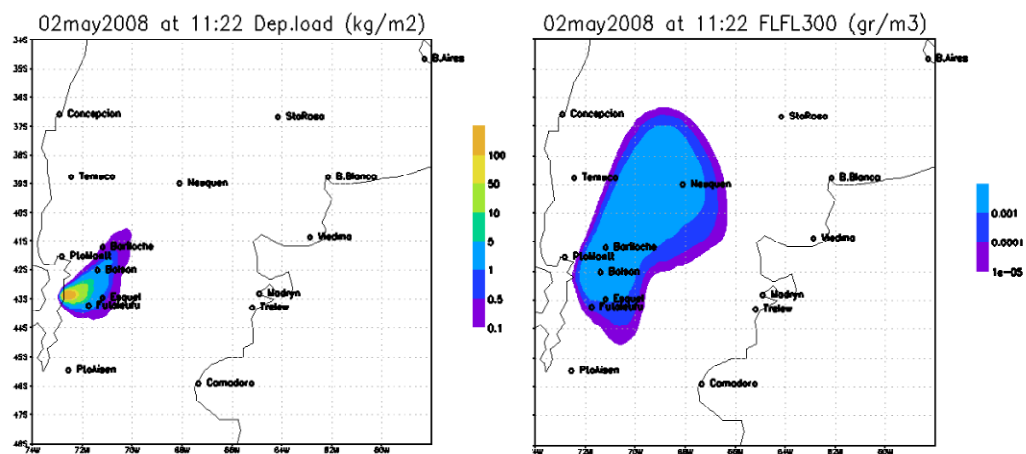


Fig 2. Deposit charge forecast (kg/m^2) (left) and concentration forecast in gr/m^3 for the 300 flight level (right), for 11:22 Z (7:22 local hour).

BIBLIOGRAPHY

- Collini, E. A., M. E. Dillon, L. Ferreira, y G. Pujol, 2010: "Estudio de la sensibilidad del modelo WRF-ARW versión SMN empleando los campos de humedad de suelo provenientes de modelos globales y de sensores remotos". AAGG 2010, Nov. 2010, Córdoba, Argentina.
- Dillon M. E., M. Armanini, A. Valdivieso, M. Suaya, y E. A. Collini, 2010: "Verificación de temperaturas extremas de otoño del modelo WRF-ARW / SMN y su comparación con el modelo ETA / SMN en el territorio Argentino", AAGG 2010, Nov. 2010, Córdoba, Argentina
- Ferreira Lorena, H. A. Salgado, C. Saulo and E. A. Collini, 2011: "Modeled and observed soil moisture variability over a region of Argentina". Aceptado para su publicación online en Atmospheric Science Letters
- Folch a, M. S. Osoreo, G. Pujol, E. A. Collini, and M. Suaya, 2011;" Evaluation of the FALL3D model using WRF-ARW fields for the 2008 Chaitén eruption". EGU 2011, Vienna, Austria, April 2011. Accepted for presentation.
- Martin P. y E. A. Collini, 2010: "Verificación de los pronósticos del WRF-ARW con observaciones de radiosondeo utilizando el MET (Model Evaluation Tool)", AAGG 2010, Nov. 2010, Córdoba, Argentina.

Experimental high-resolution forecast in a region of Argentina

Yanina García Skabar ^{1,2}, Luciano Vidal ^{1,3}, Paola Salio ^{3,4}, Matilde Nicolini ^{3,4}

¹ Servicio Meteorológico Nacional, ² Facultad de Agronomía, Universidad de Buenos Aires (UBA),

³ Departamento de Ciencias de la Atmósfera y los Océanos. FCEN. UBA,

⁴ Centro de Investigaciones del Mar y la Atmósfera, CONICET-UBA.

Argentina.e-mail: yanina@smn.gov.ar

Introduction

Heavy rainfall and other severe phenomena related to deep convection and their forecast is a major problem in different geographical regions. Subtropical South America (including the La Plata basin) is particularly affected by large and intense mesoscale convective systems (MCSs) within which severe events develop specially during the warm season. One of the main objectives is to progress in the forecast of these intense events in order to reduce related damages.

For that purpose, there is a joint effort of National Weather Service, University of Buenos Aires and Research Center of the Sea and the Atmosphere (CIMA) to design and implement an operational high-resolution forecast at the National Weather Service to contribute to improve mesoscale phenomena forecast, as convective storms. Since november 2010, an experimental operation of a high-resolution forecast in a region of Buenos Aires Province in Argentina is being carried out. Available computational resources are not enough to performed a forecast for the whole day. Forecasts are made every day and cover only the night time because several authors have shown that it is the period of greatest convective activity in the region.

Numerical model setup

Version 4.2 of Brazilian Regional Atmospheric Modeling System (BRAMS) is used to perform the forecasts; a general description of this model can be found in Freitas et al (2009) as well as online at <http://www.brams.cptec.inpe.br>. BRAMS model has been applied in the region to forecast and simulate different mesoscale phenomena and results show that it represents the observed conditions satisfactorily (García Skabar and Nicolini, 2009; Nicolini and García Skabar, 2010 and references therein). The model setup was

defined with two grids with increasing horizontal resolution of 8 and 2 km. Domains are shown in figure 1. The model uses a two way nesting technique. Vertical coordinate is terrain-following and contains 50 levels, with variable grid intervals of 20 m near surface to 1000 m at the top. The lowest level is located at 10 m from ground surface, whereas the highest level is at 26 km. The initial and boundary data are provided every 3 hours by ETA model forecast operative at the National Weather Service with 25km horizontal resolution (Suaya and Valdivieso, 2009). Model forecast are performed for 18hours, from 18 UTC to 12 UTC of the next day and are initialized with a 6 hours forecast of ETA model.

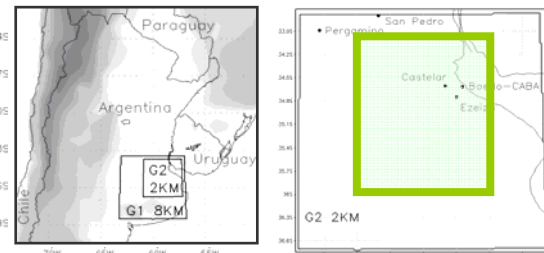


Fig.1.Left:Nested domains. Right:Detail high res. grid.

Shallow and deep convection parametrization were turned off in both grids. Microphysics parameterizations with 8 water species and bulk water scheme was applied, where mean diameter is diagnosed from forecasted mixing ratio and number concentration (Meyers et al, 1997).

Case study

During early morning of January 12, 2010 an extended convective line developed associate with a cold front that propagated over the central and northern part of Buenos Aires Province, Argentina. Related storms produced severe winds (reported gusts exceeding 30 m s^{-1}) in different locations around the city of Buenos Aires, causing material damage and even lost of lives.

For this case study model forecast performance was evaluated against measurements from radar, disdrometer, CMORPH estimations (8km-30min) and surface observations available in the region. Forecast represents a squall line reflectivity and precipitation patterns similar to observations, but

the forecast is approximately two hours later (figure 2). The same delay was observed in ETA SMN forecast that was used as initial and boundary conditions.

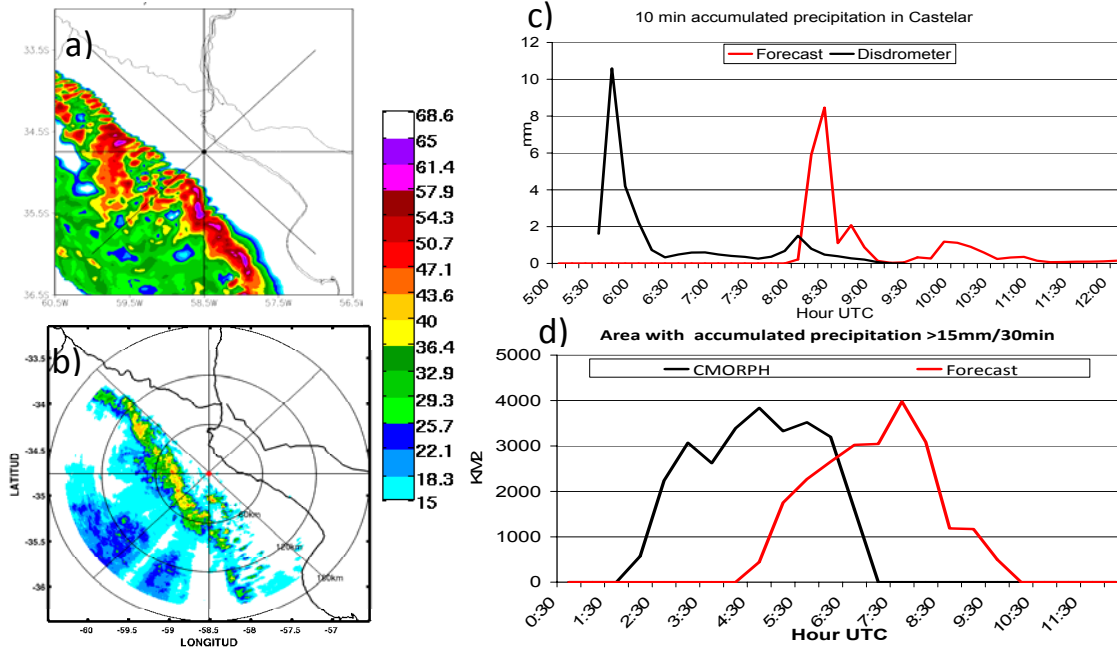


Figure 2. Reflectivity at 3km (CAPPI) a) forecast at 7 UTC and b) observed by Ezeiza ground-based radar at 5 UTC. C) 10minutes accumulated precipitation in Castelar forecast (red) and observed by disdrometer (black), d) Area where precipitation intensity is greater than 15mm/30min forecast (red) and estimated by CMORPH (black)

Future plans

Progress is needed on the development of an objective verification methodology and apply it over an extended period in an operational way. It is also important to extend the high-resolution forecast to the whole day and to other regions of the country that are also affected by severe weather.

References

- Freitas, S. R. and Coauthors, 2009: The Coupled Aerosol and Tracer Transport model to the Brazilian developments on the Regional Atmospheric Modeling System (CATT-BRAMS). Part 1: Model description and evaluation. *Atmos. Chem. Phys.*, 9, 2843–2861.
- García Skabar, Y. and M. Nicolini, 2009: Enriched Analyses with Assimilation of SALLJEX Data.

Journal of Applied Meteorology and Climatology, Vol.48, pág. 2425-2440.

Meyers, M. P., R. L. Walko, J. Y. Harrington, and W. R. Cotton, 1997: New RAMS cloud microphysics parameterization. Part II. The two-moment scheme. *Atmos. Res.*, 45, 3–39.

Nicolini, M. and Y. García Skabar, 2010: Diurnal cycle in convergence patterns in the boundary layer east of the Andes and convection. In press at *Atmospheric Research*.

Suaya, M., and R. Valdivieso, 2009: ETA SMN MODEL: USAGE, EXPERIENCES AND RESULTS DURING 2003-2008. Proceedings Congremet X/Climet XII, 2009, Published in spanish.

Acknowledgements: This research is supported by the following grants: PIDDEF 47/2010, UBACYT X159, ANPCyT PICT 2007-00355, CONICET-PIP2009 Nicolini. Authors would like to thank to CPTEC for provide the disdrometer and INTA and GCBA their observations.

Trial operation of the Local Forecast Model at JMA

Youichi Hirahara, Junichi Ishida, and Takahisa Ishimizu

Numerical Prediction Division, Japan Meteorological Agency

1-3-4 Otemachi, Chiyoda-ku, Tokyo 100-8122, Japan

(E-mail: hiraharayo@met.kishou.go.jp)

1. Introduction

The Japan Meteorological Agency (JMA) is developing the Local Forecast Model (LFM) – an NWP model with a horizontal grid spacing of 2 km – to contribute to aviation weather forecasts around airports and provide more detailed information for the prevention of disasters caused by heavy rainfall. In advance of the LFM's scheduled introduction to actual operation in 2012, a period of trial operation was started in November 2010. In this trial, the model is run eight times a day with a forecast domain covering the middle and western parts of Japan (Fig. 1), and test products are provided to aviation users for evaluation.

2. Trial operation specifications

The specifications of the trial operation are summarized in Table 1. The LFM is based on JMA's non-hydrostatic model (JMA-NHM: Saito et al. 2006) in the same way as the operational Mesoscale Model (MSM: Hara et al. 2007) with a horizontal grid spacing of 5 km. The MSM uses a cumulus parameterization scheme in conjunction with a bulk-type microphysics scheme, while the LFM uses only a microphysics scheme to explicitly represent moist convection.

3. Verification results

Ahead of the trial operation, the LFM was experimentally operated in the same domain as the trial operation (Ishimizu et al. 2010). This section outlines verification results for operation during the period from June 2010 to August 2010. Figure 2 shows the bias score (BS) and the equitable threat score (ETS) of precipitation forecasts against Radar/Raingauge-Analyzed precipitation. The BS for precipitation averaged for each 20-km square mesh shows that the LFM tends to overestimate precipitation areas for intense rainfall (Fig. 2 a). In contrast, the BS for maximum precipitation in each 20-km square mesh shows that the LFM is closer to unity than that in MSM forecasts (Fig. 2 c). The ETS for the maximum precipitation in each 20-km square mesh shows that the LFM forecasts precipitation more accurately than the MSM (Fig. 2 d). These tendencies have also been detected for smaller-domain operation (Nakayama et al. 2007; Takenouchi et al. 2008). The above-mentioned results show that the LFM is able to appropriately forecast the maximum intensity of heavy rainfall. Figures 3 and 4 show verification of wind speeds in LFM and MSM forecasts against the Wind Profiler Network and Data Acquisition System (WINDAS), which covers the islands of Japan with a special resolution of 130 km on average. The wind speed biases show the same tendency in both models, and the root mean square error is smaller in LFM forecasts than in MSM results at altitudes below 1 km. This indicates the improvement of lower atmosphere winds as desired for aviation weather forecasts around airports.

4. Future plans

JMA plans hourly operation of the LFM for the domain covering the islands of Japan from 2013. As the verification results obtained here indicate that the LFM tends to overestimate forecasts of heavy rainfall, we will investigate ways to improve the related physical processes.

References

- Saito, K., T. Fujita, Y. Yamada, J. Ishida, Y. Kumagai, K. Aranami, S. Ohmori, R. Nagasawa, S. Kumagai, C. Muroi, T. Kato, H. Eito and Y. Yamazaki, 2006: The operational JMA Nonhydrostatic Mesoscale Model. *Mon. Wea. Rev.*, **134**, 1266 – 1298.
- Hara, T., K. Aranami, R. Nagasawa, M. Narita, T. Segawa, D. Miura, Y. Honda, H. Nakayama and K. Takenouchi, 2007: Upgrade of the operational JMA non-hydrostatic mesoscale model. *CAS/JSC WGNE Res. Activ. Atmos. Oceanic Modell.*, **37**, 0511 – 0512.

- Ishimizu, T., M. Ujiie, 2010: Experimental operation of a high-resolution local forecast model at JMA (3). *CAS/JSC WGNE Res. Activ. Atmos. Oceanic Modell.*, **40**, 0513 – 0514.
- Nakayama, H., Y. Ishikawa, T. Fujita and K. Takenouchi, 2007: Experimental operation of a high-resolution local forecast model at JMA. *CAS/JSC WGNE Res. Activ. Atmos. Oceanic Modell.*, **37**, 0519 – 0520.
- Takenouchi, K., H. Kurahashi, T. Fujita and K. Aranami, 2008: Experimental operation of a high-resolution local forecast model at JMA (2). *CAS/JSC WGNE Res. Activ. Atmos. Oceanic Modell.*, **38**, 0523 – 0524.

Table 1. Specifications of the LFM for trial operation

Horizontal mesh (grid spacing)	800 x 550 (2 km)
Vertical layers	60 (top level: 20 km)
Forecast period/frequency	9 hours, 8 times/day
Lateral boundary	MSM
Data assimilation	Rapid update cycle using JNoVA-3DVar
Moist physics	3 ice bulk microphysics (snow, ice, graupel)
Cumulus parameterization	Not used



Fig. 1: Model domains

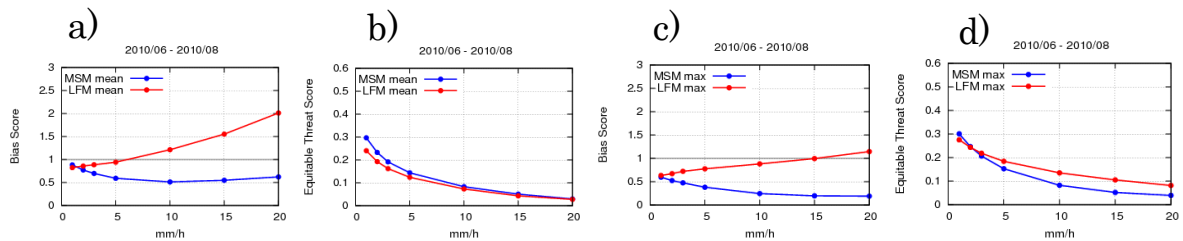


Fig. 2: (a) Bias scores for hourly rainfall amounts according to the LFM (red line) and the MSM (blue line) against the threshold of rainfall intensity (averaged for each 20-km square mesh on land and over the sea in coastal areas); (b) as per (a), but for equitable threat score (ETS); (c) as per (a), but for the maximum in each 20-km square mesh; (d) as per (c), but for ETS

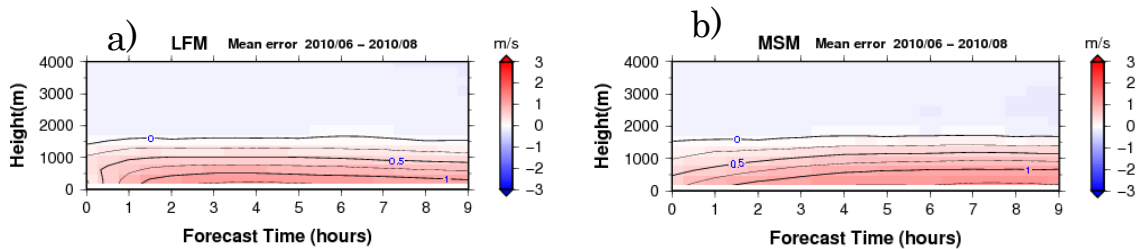


Fig. 3: Mean error of wind speed against WINDAS: (a) LFM; (b) MSM

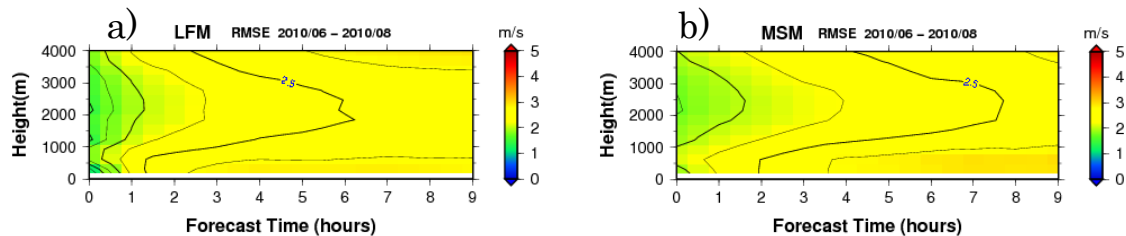


Fig. 4: RMSE of wind speed against WINDAS: (a) LFM; (b) MSM

Increase of COSMO–LEPS horizontal resolution: impact on the prediction of precipitation events

ANDREA MONTANI, C. MARSIGLI AND T. PACCAGNELLA

ARPA–SIMC, Bologna, Italy

Introduction

In the framework of limited–area ensemble forecasting, the COSMO–LEPS system (Montani et al., 2003) was the first mesoscale ensemble application running on a daily basis in Europe since November 2002. A number of system upgrades had a positive impact on COSMO–LEPS forecast skill of precipitation in the short and early medium–range, documented by Montani et al., 2011. As computer power resources increase, it was investigated the extent to which an increase in horizontal resolution of COSMO–LEPS runs could have a benefit on the probabilistic prediction of those surface fields, like precipitation and 2–metre temperature, heavily affected by orography and mesoscale processes. For this reason, a number of system upgrades were tested and their impact was studied, focusing the attention to the performance of COSMO–LEPS for heavy precipitation events. More precisely, the following modifications were introduced:

- increase of the horizontal resolution from 10 to 7 km;
- enlargement of the integration domain so as cover Central and Southern Europe;
- introduction of new “stochastic” perturbations in COSMO–LEPS runs.

From June to November 2009, both the operational system (referred to as “oper”) as well as the new one (referred to as “test”) were run in parallel and the performance of both systems were analysed considering the probabilistic prediction of 12–hour accumulated precipitation exceeding a number of thresholds for several forecast ranges.

Methodology and results

As for observations, we use the data obtained from the SYNOP reports available on the Global Telecommunication System (GTS). In order to assess the skill of the system over complex topography, verification is first performed over the domain ranging from 43N to 50N and from 2E to 18E, the MAP D-PHASE area (Mesoscale Alpine Programme, Demonstration of Probabilistic Hydrological and Atmospheric Simulation of flood Events in the alpine region). Within this domain (referred to as “mapdom”), a fixed list of 412 SYNOP stations is considered and the relative reports in terms of total precipitation are used to evaluate the COSMO–LEPS skill. In addition to this, it has been also considered a second (larger) domain, which includes approximately the full COSMO–LEPS domain, ranging from 35N to 58N and from 10W to 30E. Within this further domain (referred to as “fulldom”), a list of 1542 stations is taken and the performance of “oper” and “test” is also assessed. As for the comparison of model forecasts against SYNOP reports, we select the grid point closest to the observation. The performance of COSMO–LEPS is examined for 6 different thresholds: 1, 5, 10, 15, 25 and 50 mm/12h. The verification is performed over a 6–month period, from June to November 2009. Over this period, the following probabilistic (scores Marsigli et al., 2008) are presented: the Ranked Probability Skill Score (RPSS) and the Percentage of Outliers (OUTL).

The skill of the two systems in terms of prediction of 12–hour accumulated precipitation is summarised in Fig. 1, where the RPSS is plotted (left panel) against the forecast range for both

“oper” and “test” configurations. It can be noticed that “test” COSMO-LEPS has higher RPSS for all forecast ranges. The difference between the two systems is consistent throughout the full forecast range, up to day 5, with a larger gap in favour of “test” COSMO-LEPS more evident for the first two days of integrations. This holds when verification is performed either in the

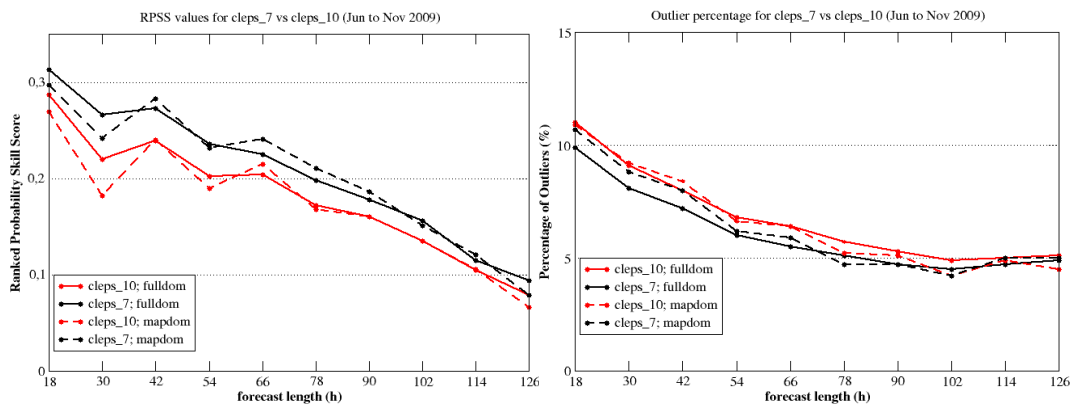


Figure 1: Ranked Probability Skill Score (left panel) and Percentage of Outliers (right panel) for “oper” (red) and “test” (black) COSMO-LEPS. Solid (dashed) lines refer to scores over the “fulldom” (“mapdom”). Scores are calculated over the period June–November 2009.

Alpine area (dashed lines, relative to “mapdom”) or over the entire integration domain (solid lines, relative to “fulldom”). Then, the attention is focused on the ability of the “test” system to reduce the number of outliers with respect to “oper”, thanks to the higher resolution as well as to the introduction of new perturbations which should ensure a larger spread among “test” forecasts. The right panel of Fig. 1 shows that, in the 7-km system (black lines), the OUTL is reduced for all forecast ranges, except the longest one, with respect to the operational system. The impact is more evident over the “fulldom”, where the higher-resolution system outperforms “oper” with a 12-hour gain in predictability. It can also be noticed that, for all configuration and verification networks, there is a sort of “plateau” at about 5% of outliers, which seems, at the moment, a limit for the number of outliers in COSMO-LEPS systems.

The above-mentioned results show the potential of the higher-resolution COSMO-LEPS, which can provide more accurate rainfall forecasts, thanks to a better description of orographic and mesoscale-related processes. In addition to this, the introduction of new model perturbations proved to have a positive effect on the forecast skill of the ensemble system. Following the indications provided by the different probabilistic scores, the 7-km COSMO-LEPS was implemented operationally in December 2009 and has been running on a daily basis since then. As for the future, it is envisaged to continue the systematic verification of the system, to monitor the added value of the higher resolution in the ensemble runs and to study new possible ameliorations.

References

- Marsigli C., Montani A., Paccagnella T., 2008. A spatial verification method applied to the evaluation of high-resolution ensemble forecasts. *Met. Appl.*, **15**, 125–143.
- Montani A., Capaldo M., Cesari D., Marsigli C., Modigliani U., Nerozzi F., Paccagnella T., Tibaldi S., 2003. Operational limited-area ensemble forecasts based on the ‘Lokal Modell’. ECMWF Newsletter No. 98. Available from: European Centre for Medium-Range Weather Forecasts, Shinfield Park, Reading RG2 9AX, UK.
- Montani A., Cesari D., Marsigli C., Paccagnella T., 2011. Seven years of activity in the field of mesoscale ensemble forecasting by the COSMO-LEPS system: main achievements and open challenges. *Tellus A*, in print. DOI: 10.1111/j.1600-0870.2010.00499.x

A mesoscale ensemble prediction system using singular vector methods

Kosuke Ono* Yuki Honda* and Masaru Kunii**

*Numerical Prediction Division, Japan Meteorological Agency, Tokyo, Japan

**Department of Atmospheric and Oceanic Science, University of Maryland, College Park, USA

E-mail: kou.ono@met.kishou.go.jp

We have been developing a mesoscale ensemble prediction system (MEPS) using singular vector (SV) methods for the provision of probabilistic information and multi-scenarios in operational mesoscale forecasting (MSM) since 2007. In order to improve the related probability scores, we developed a method of generating initial perturbations (IPs) by blending two mesoscale SVs (MSVs) (Ono et al. 2010). However, the IP amplitude is too large in regions where two MSVs turn in the same direction because this method involves simple addition of the two MSVs. It is also necessary to add a global SV (GSV) to the two MSVs to account for the uncertainty of synoptic scale phenomena. Accordingly, we have developed a new IP method in which multi-scale IPs are generated by blending three SVs using the variance minimum method (Yamaguchi et al. 2009), which rotates all SVs so that IPs have a broader structure. We conducted a daily mesoscale ensemble forecasting experiment using this IP method in the latter half of 2010 to ascertain its level of performance.

Table 1 lists the details of the SV calculations and the subsequent ensemble forecasts for the daily experiment. MSVs are calculated using the tangent linear and its adjoint model (TL/AD) based on JMA's nonhydrostatic model (JMA-NHM) (Honda et al.2005). GSVs are calculated using the TL/AD of the JMA's global spectral model. The lateral boundary is perturbed using the outputs of JMA's operational weekly ensemble prediction. In ensemble forecasting, the ensemble size is 11 (including control forecasting), and the horizontal resolution of JMA-NHM is set to 20 km to reduce computational costs.

A case of the heavy rain caused by Baiu front at 00 UTC on 03 July 2010 (T+6) is shown in Figure 1. Some ensemble members forecast heavy rain near the front that the control forecast does not forecast. However, at the southern side of the front, no member forecasts the heavy rain. The daily experiment suggests that this system forecasts heavy rain associated with disturbances such as fronts and low pressure systems well.

Figure 2 shows the rank histograms for wind speed against sonde observations around Japan (verification period: 03 July - 13 September 2010; total: 59 cases). It can be seen that the ensemble spread at the surface is too small over the forecast period. One of the main reasons for this is that the MSV amplitude is small near the surface. On the other hand, the ensemble spreads at 850 hPa and 500 hPa are more appropriate. Corresponding to these characteristics, the improvement rate of the ensemble mean forecast against the control forecast at upper levels is better than that near the surface (Figure 3). These characteristics are also confirmed for other elements.

Figure 4 shows reliability diagrams for three-hour accumulated precipitation. It can be seen that at higher levels of precipitation probability, this system tends to overforecast precipitation, i.e., most ensemble members forecast the same precipitation.

In order to improve the performance of this system (especially the ensemble spread near the surface and the precipitation score), we plan to develop a physics perturbation method and reinforce the horizontal resolution and ensemble size for ensemble forecasting on the next super computer system at the JMA.

Table 1 Ensemble spread of three-hour accumulated precipitation [mm/3h].

SV calculation			Ensemble forecast		
Type	MSV40	MSV80	GSV	Model	JMA-NHM
dx	40 km	80 km	180 km	dx	20 km
Optimization time	6 h	15 h	24 h	Ensemble size	11
Norm	Moist total energy	Moist total energy	Dry total energy	Forecast time	36 h
Number	10	5	5	Initial time	18 UTC

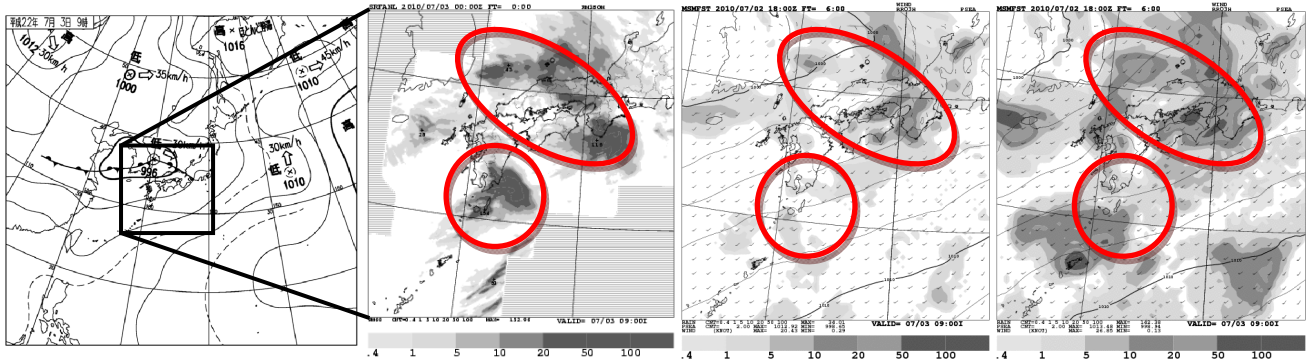


Fig1. Weather chart and three-hour accumulated precipitation at 00UTC on 03 July, 2010 (observation, control forecast and maximum precipitation in all ensemble members, T+6).

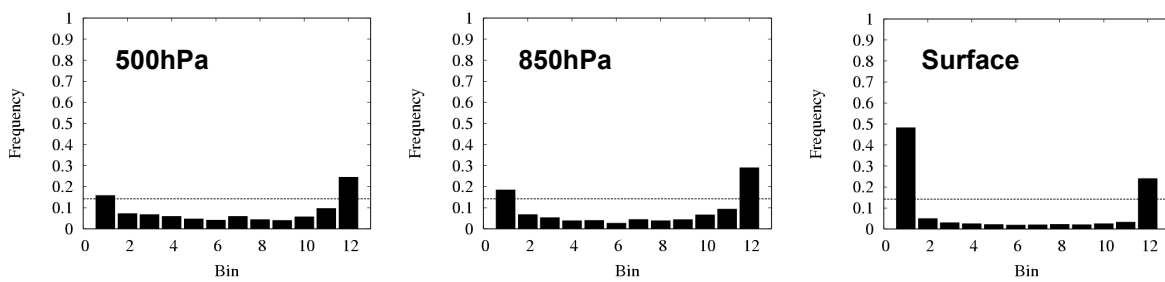


Fig2. Rank histograms of wind speed (500 hPa, 850hPa and surface, T+30).

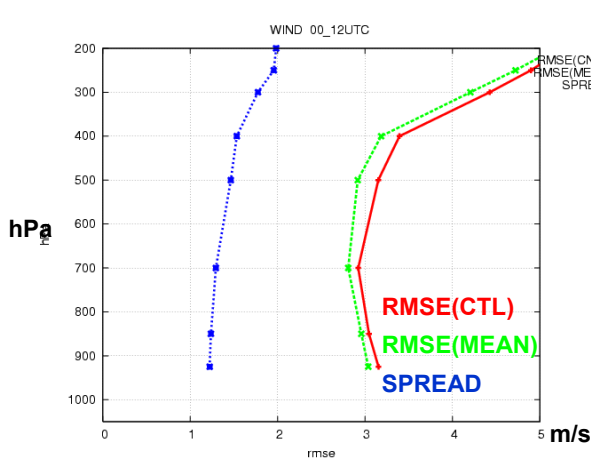


Fig3. Root mean square error and ensemble spread of wind speed (T+30)..

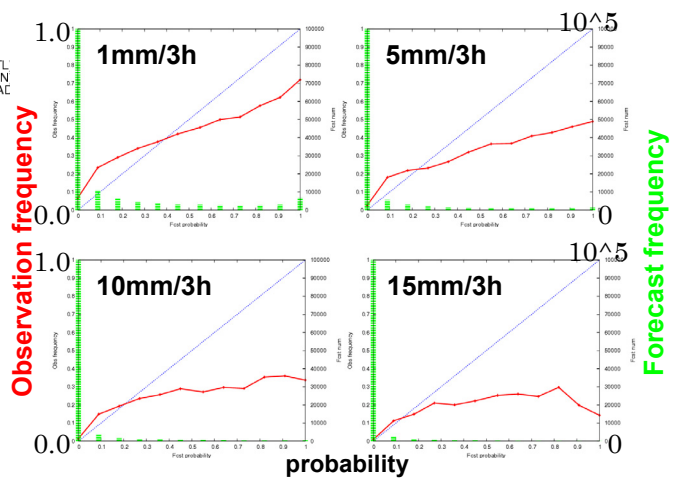


Fig4. Reliability diagrams of three-hour accumulated precipitation (T+12).

References

- Honda, Y., and coauthors, 2005: A pre-operational variational data assimilation system for a nonhydrostatic model at Japan Meteorological Agency: Formulation and preliminary results. *Q.J. R. Meteorol. Soc.*, **131**, 3465-3475.
- Ono, K., Y. Honda and M. Kunii, 2010: Development of a mesoscale ensemble prediction system using a singular vector method. *CAS/JSC WGN Res. Act. Atmos. Ocea. Modell.* **40**, 5.17-5.18.
- Yamaguchi, M., and coauthors, 2009: Typhoon ensemble prediction system developed at the Japan Meteorological Agency. *Mon. Wea. Rev.*, **137**, 2592-2604.

Investigating the role of soil moisture gradients on extreme precipitation over Southeastern South America

R. C. Ruscica ⁽¹⁾, A. A. Sörensson ⁽¹⁾, C. G. Menéndez ^(1,2)

⁽¹⁾ Centro de Investigaciones del Mar y la Atmósfera, CONICET/UBA, Buenos Aires, Argentina.

⁽²⁾ DCAO, FCEN, Universidad de Buenos Aires, Argentina.

ruscica@cima.fcen.uba.ar

Introduction

Soil moisture plays an important and complex role in the climate predictability, since it forces the atmosphere in different spatial and time scales. Its interaction with the precipitation (couplings, positive/negative feedbacks) has been and remains a subject of study connected to the hydrological cycle, using observational and satellite data and climate models (e.g. Sörensson and Menéndez, 2010). The influence of the soil moisture horizontal contrasts on precipitation in different spatial scales has been suggested in some articles (e.g. Emori, 1998; Frye and Mote, 2009; Wolters et al., 2010). In a new approach, we investigate the possible connection between the soil moisture horizontal gradient and extreme precipitation, using a regional climate model over Southeastern South America (SESA, Fig.1), during the development of the South American Monsoon System 1992-93.

Model and Methodology

The Rossby Centre Atmospheric regional model RCA3-E (Samuelsson et al., 2011) was employed. This model version has a better representation of the land surface than earlier versions. The land surface scheme has two soil moisture layers, the top one being 7 cm deep and the deep one was determined by Ecoclimap (Champeaux et al., 2005) at each grid point. The model domain covers the South American continent, and is based on a rotated grid system with a horizontal resolution of 0.5° and 24 unevenly spaced sigma levels in the vertical with the five lowest levels below 900 hPa. All initial and boundary conditions are from ECMWF Re-Analysis (ERA-40, Uppala et al., 2005).

An ensemble of ten four-months continuous simulations was created, starting from different initial dates. Each member extends from November 1 1992 to March 31 1993 (neutral ENSO conditions). In order to initialize the regional model with the atmosphere–soil moisture in equilibrium, the soil moisture initial conditions are set to the soil moisture fields of corresponding initial date from a RCA3-E/ERA-40 integration initialized on September 1, 1990. The analysis is focused on the SESA region during DJF, region and period in which RCA-E has a good performance in the mean precipitation (Fig.1).

We identified at each grid point the extreme precipitation events defined as the percentile 95 of the ensemble, and we perform a composite of the “day 0” (mean precipitation of days in which rainfall equals or exceeds that percentile). We also computed time-lag composite fields of the absolute value of the top soil moisture horizontal gradient for previous days (day -1). Then we calculated fields of relative anomalies (defined as the difference between the composite and the mean value, divided by the mean value) of precipitation for “day 0” and those of soil moisture gradient for “day -1”.

Results

Over the region, rainfall extremes are associated with intense convective storms (e.g. Zipser et al., 2006). We speculate that the surface soil moisture heterogeneities would favor the development of heavy precipitation events. In our experiment we find that, on the day before the extreme precipitation event, the spatial heterogeneity of soil moisture tends to be enhanced relative to that in the mean field ensemble. This is shown in Fig.3 where there are mostly positive relative anomalies of soil moisture gradient, with large surface contrasts on day -1 over parts of eastern Argentina, southern Brazil, Uruguay, and along the coasts (blue dots, values close to unity indicating that the horizontal contrast doubles the mean value). In general, these maxima are located in regions where precipitation anomalies are high (greater than 10 times the mean, Fig.2). In the “day -2” (not shown) no significant changes are seen on the gradient’s map. As expected, the relative anomalies of soil moisture gradient in the “day 0” are mostly negative, because the heavy rainfalls tend to homogenize the soil moisture field. The future work includes inquiring into the physical processes involved and carrying out additional ensembles for other years.

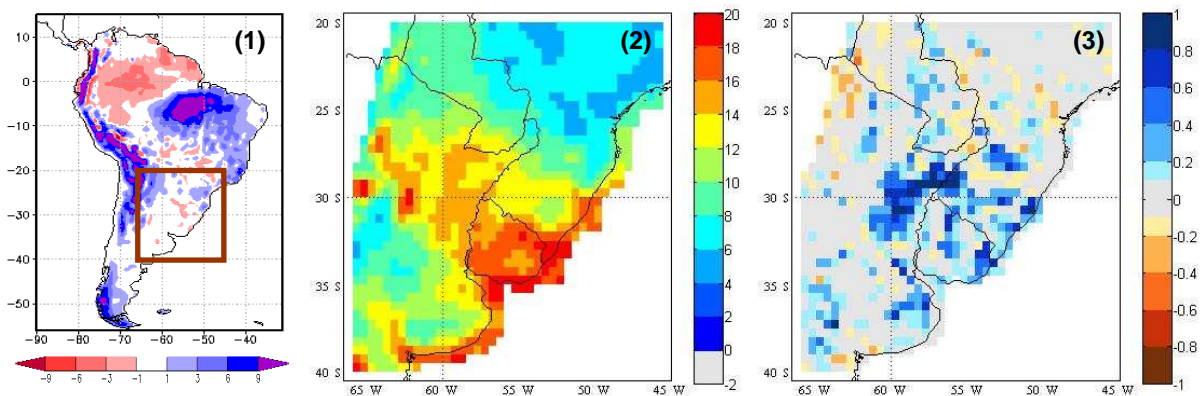


Fig (1): Mean Precipitation Bias (RCA3-E minus CRU) in DJF 1980-99 (mm/day) and studied SESA region inside box. Fig (2): Relative anomalies of precipitation, “day 0”. Fig (3): Relative anomalies of absolute value of top soil moisture horizontal gradient, “day -1”. Ocean and altitudes higher than 1200 m are masked.

References

- Champeaux, J.L., Masson, V. and Chauvin, F. 2005. ECOCLIMAP: a global database of land surface parameters at 1 km resolution. *Met.Appl.* 12, 29–32.
- Emori, S. 1998. The interaction of cumulus convection with soil moisture distribution: An idealized simulation, *J. Geophys. Res.*, 103, 8873–8884.
- Frye, John D., Thomas L. Mote. 2009: The Synergistic Relationship between Soil Moisture and the Low-Level Jet and Its Role on the Prestorm Environment in the Southern Great Plains. *J. Appl. Mete.Climatol.*, 49,775–791.
- Samuelsson, P., Jones, C., Willén, U., Gollvik, S., Hansson, U. and coauthors. 2011. The Rossby Centre Regional Climate Model RCA3: model description and performance. *Tellus* 63A, 4–23.
- Sörensson, A. A. and Menéndez, C. G. 2011. Summer soil–precipitation coupling in South America. *Tellus A*, 63: 56–68. doi: 10.1111/j.1600-0870.2010.00468.x
- Uppala, S.M., Kållberg, P.W., Simmons, A.J., Andrae, U., da Costa Bechtold, V. and co-authors. 2005. The ERA-40 re-analysis. *Quart J. R. Meteorol. Soc.* 131, 2961–3012.
- Wolters, D., van Heerwaarden, C. C., de Arellano, J. V.-G., Cappelaere, B. and Ramier, D. 2010. Effects of soil moisture gradients on the path and the intensity of a West African squall line. *Quart. J. R. Meteorol. Soc.*, 136: 2162–2175. doi: 10.1002/qj.712.
- Zipser, E. J., Cecil, D. J., Liu, C., Nesbitt, S. W. and Yorty, D. P. 2006. Where are the most intense thunderstorms on Earth?. *Bull. Am. Meteorol. Soc.* 87, 1057–1071.

Next generation supercomputer project toward cloud resolving NWP

**Kazuo SAITO¹, Hiromu SEKO¹, Tohru KURODA^{2,1}, Tadashi FUJITA³,
Takuya KAWABATA¹, Kazumasa AONASHI¹ and Tadashi TSUYUKI¹**

¹*Meteorological Research Institute, Tsukuba, Ibaraki 305-0052, Japan; ksaito@mri-jma.go.jp*

²*Japan Agency for Marine-Earth Science and Technology,* ³*Numerical Prediction Division, Japan Meteorological Agency*

Accuracy of the quantitative precipitation forecast of operational mesoscale numerical weather prediction (NWP) has been remarkably improved in recent years, but precise prediction of heavy rainfalls in unstable atmospheric conditions is still a difficult and challenging subject. Several studies such as development of a cloud-resolving data assimilation system, assimilation of mesoscale remote-sensing observation data (e.g. GPS perceptible water vapor), and development of mesoscale ensemble prediction systems, have been conducted at the Meteorological Research Institute (MRI). Computer resource and observation data are keys to realize full-scale dynamical and probabilistic forecasts of local heavy rainfalls for disaster prevention.

The next-generation supercomputer project, “High-Performance Computing Infrastructure (HPCI) project”, is being carried out by RIKEN, with partners in industry, universities, and government institutions, under an initiative by the Ministry of Education, Culture, Sports, Science and Technology (MEXT) of Japan. The supercomputer center is being built in the city of Kobe, western Japan (http://www.aics.riken.jp/index_e.html). The supercomputer ‘K’, in which 80,000 nodes (640,000 cores) of the FUJITSU SAPARC64 processor are installed, will start its operation in April 2011, and the whole system that attains 10 Pflops will be completed in the autumn of 2012. The project consists of five strategic research fields (Life science & medicine, New material & energy, Disaster prevention, Engineering, and Matter & universe), and a five-year research plan of high performance NWP with cloud resolving ensemble data assimilation has been endorsed as one of the sub-project of the Field 3 on the ‘K’ supercomputer.

The sub-project on mesoscale NWP has following three subjects:

- a) Development of a cloud resolving 4 dimensional data assimilation system.
- b) Development and validation of a cloud resolving ensemble analysis forecast system.
- c) Basic research using very high resolution atmospheric models

The goal of Subject a) is to dynamically predict local heavy rainfalls with deep convection by assimilating dense observation data. A field campaign in the Tokyo metropolitan area will be conducted by MRI and the National Research Institute for Earth Science and Disaster Prevention (NIED) in the summers of 2011-2013 as a possible international test-bed for deep convection. Advanced data assimilation methods such as 4DVAR, LETKF and Ensemble VAR based on nonhydrostatic models in Japan have been developed and applied to case studies of cloud resolving forecast experiments of precipitation. (e.g., Kawabata et al., 2011; Seko et al., 2011; Aonashi and Eito, 2011).

The goal of Subject b) is to show plausibility of the probabilistic quantitative forecast of heavy rainfalls for disaster prevention by cloud resolving ensemble NWP. A NHM-LETKF system using incremental approach (Fig. 1) has been developed at JMA (Fujita et al., 2011) and has been modified at MRI expecting the application to the ‘K’ computer (Kuroda et al., 2011). Figure 2 shows the ensemble spread of temperature (T) and horizontal wind (U) at 500 hPa by the incremental NHM-LETKF. Amplitude of ensemble spreads is kept significant near the lateral boundaries by introduction of lateral boundary perturbations, of which method was developed at the WWRP B08RDP project (Saito et al., 2011).

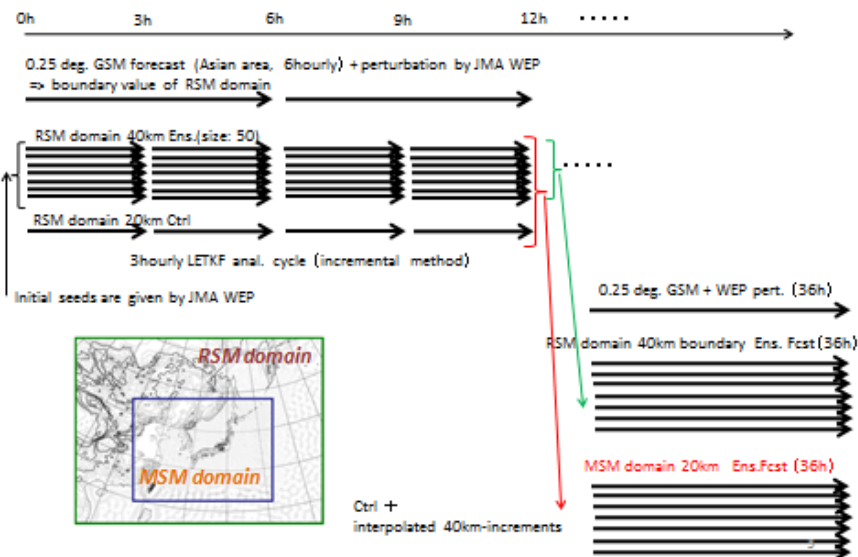


Fig. 1. Schematic diagram of the incremental NHM-LETKF. After Kuroda et al. (2011).

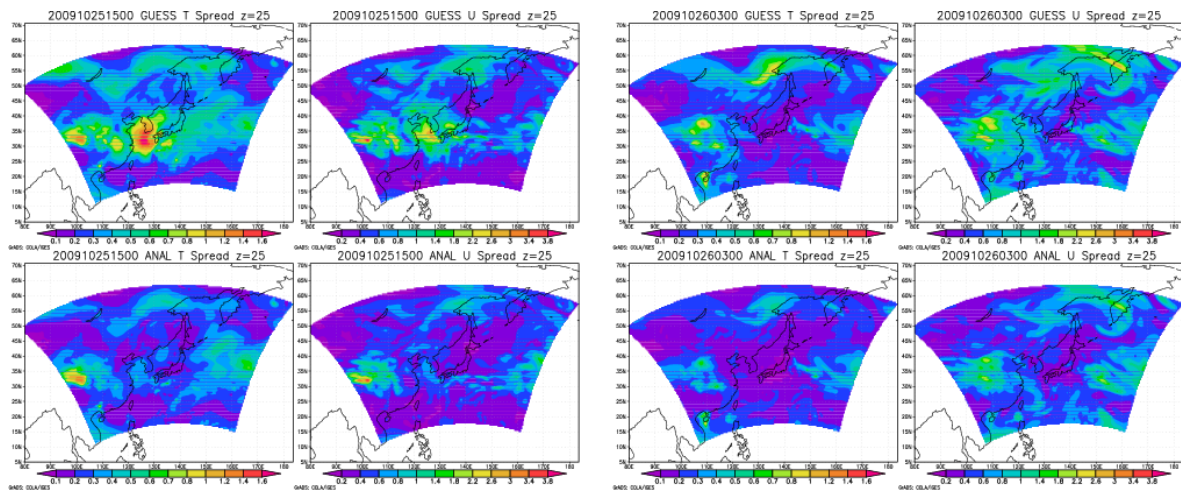


Fig. 2. Ensemble spread of the first guess fields (upper) and the analysis fields (lower) for temperature (T) and horizontal wind (U) at 500 hPa by the incremental NHM-LETKF. Left) 15 UTC 25 October 2009. Right) 03 UTC 26 October 2009. After Kuroda et al. (2011).

References

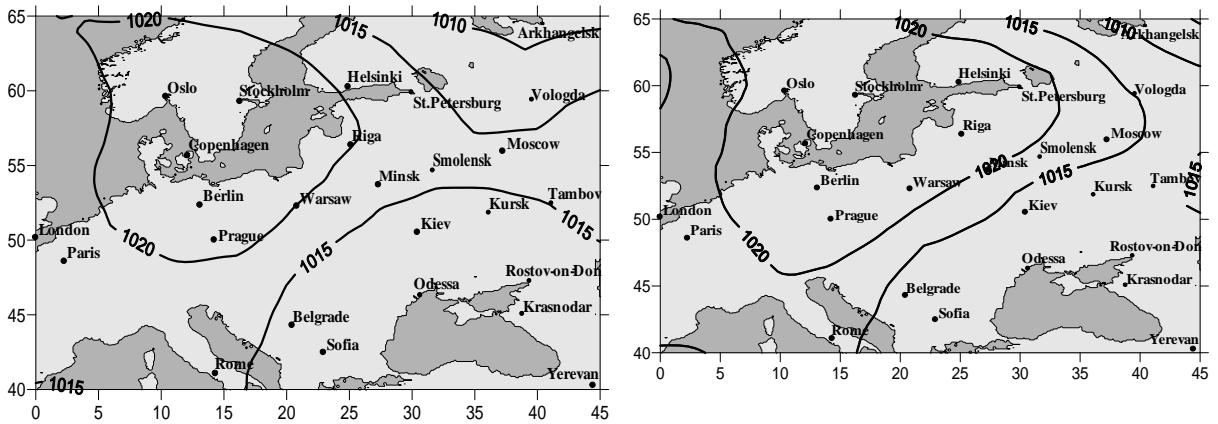
- Aonashi and Eito, 2011: Displaced ensemble variational assimilation method to incorporate microwave imager data into a cloud-resolving model. *J. Meteor. Soc. Japan*, **89**. (in press)
- Fujita, T., T. Kuroda, H. Seko and K. Saito, 2011: Development of a meso ensemble data assimilation system. *Presentation, 2011 Meeting on the Study of Advanced Data Assimilation and Cloud Resolving Ensemble Technique for Prediction of Local Heavy Rainfall*. (available on line at ftp://ftp.mri-jma.go.jp/ez0do01/Kakenhi_H21/H22b/Fujita_20110228.pdf)
- Kawabata, T., T. Kuroda, H. Seko and K. Saito, 2011: A cloud-resolving 4D-Var assimilation experiment for a local heavy rainfall event in the Tokyo metropolitan area. *Mon. Wea. Rev.*, **139**. (in press)
- Kuroda, T., T. Fujita, H. Seko and K. Saito, 2011: Development and near future utilization of incremental LETKF data assimilation system at MRI. *Presentation, 2011 Meeting on the Study of Advanced Data Assimilation and Cloud Resolving Ensemble Technique for Prediction of Local Heavy Rainfall*. (available on line at ftp://ftp.mri-jma.go.jp/ez0do01/Kakenhi_H21/H22b/Kuroda_20111028.pdf)
- Saito, K., H. Seko, M. Kunii and T. Miyoshi, 2011: Effect of lateral boundary perturbations on the breeding method and the local ensemble transform Kalman filter for mesoscale ensemble prediction. *Tellus*. (submitted)
- Seko, H., T. Miyoshi, Y. Shoji and K. Saito, 2011: A data assimilation experiment of PWV using the LETKF system -Intense rainfall event on 28 July 2008-. *Tellus*, **63A**. (in press)

Forecast of Meteorological Variables and Turbulence Parameters

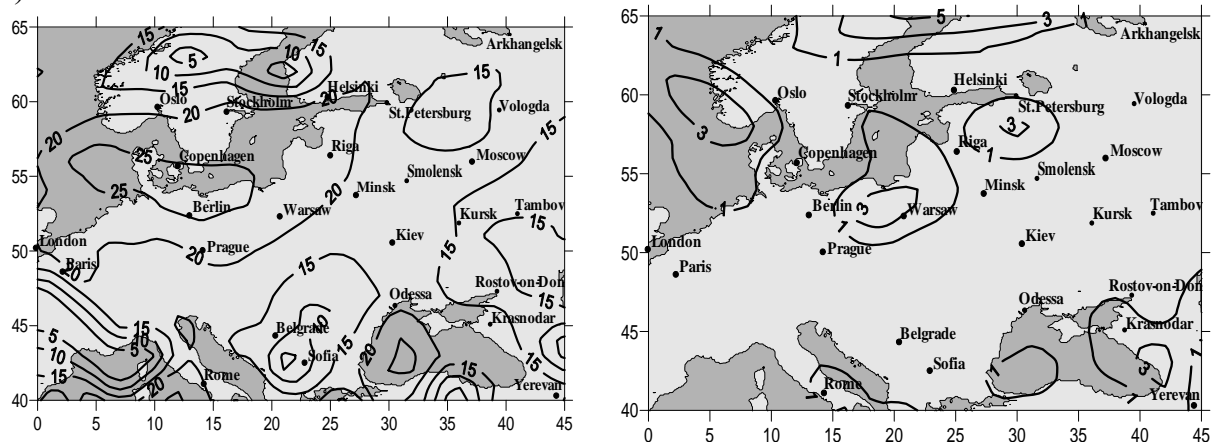
Shnaydman V New Jersey State University-Rutgers, USA volf@envsci.rutgers.edu
 Berkovitch L., Tkacheva Ju. Hydro-meteorological Research Center, Russia.

The fields of the wind, temperatures, specific humidity and the geopotential on the basic isobaric surfaces, as well as ground temperature and specific humidity are predicted in hemispheric model of Hydro-meteorological center of Russia. The prediction is based on the solution of the equations of hydro thermodynamics and the description of turbulent processes are carried out under the simplified closure boundary layer one-dimensional model (1). The calculated fields are used for the forecasts in the points of Central Russia area, and vertical structures of a wind and vertical turbulent coefficient are applied in laboratory of unfavorable meteorological condition warning. The results obtained showed that the model with inclusion of the three-dimensional equations for turbulent kinetic energy and dissipation have future before one. The developed research forecast model used the currently available linearization, thermal stratification influence valuation and time integration method in the turbulence closure equations (2). This improved forecast model is testing now. The sample of testing results for the predicted fields and vertical distribution is given in the figures. The maps of predicted values: surface pressure a), vertical turbulence coefficient b), wind module c). Left forecast is for 12 hours, right forecast is for 24 hours.

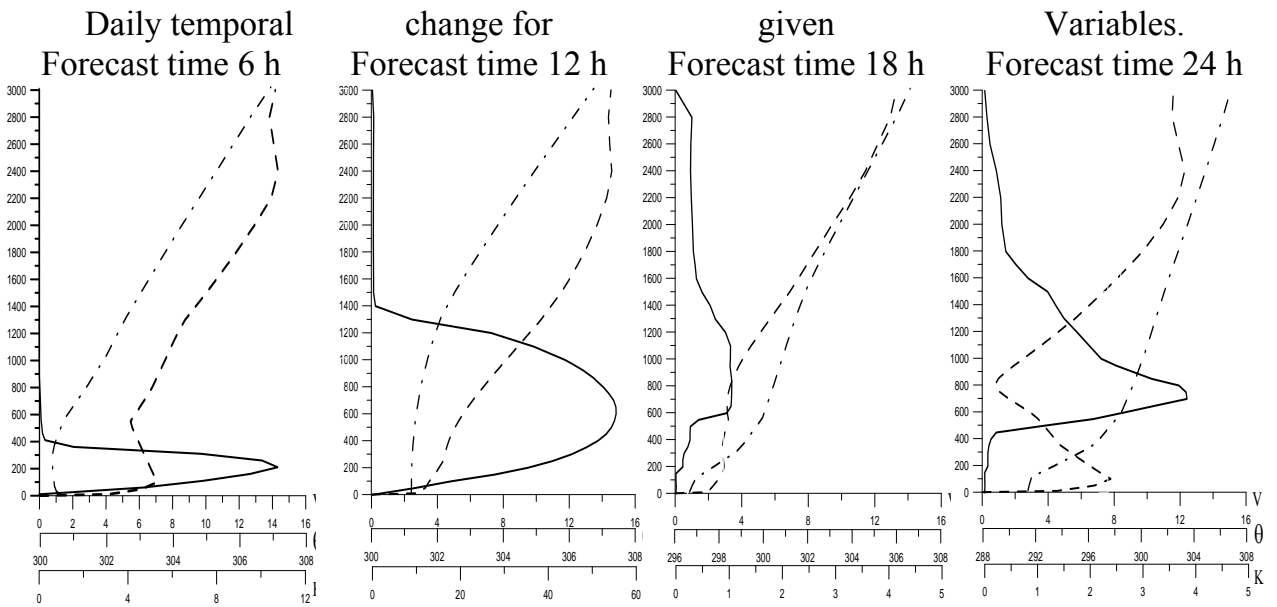
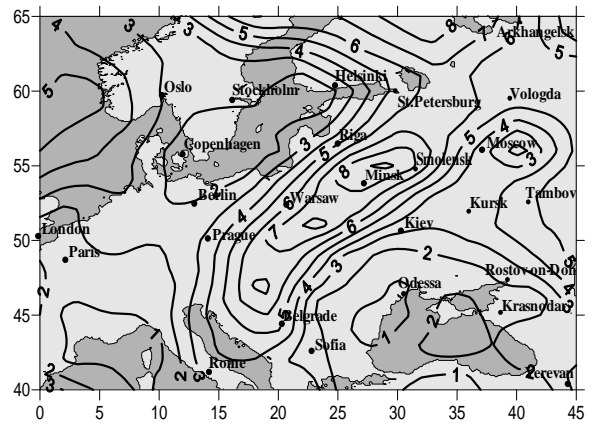
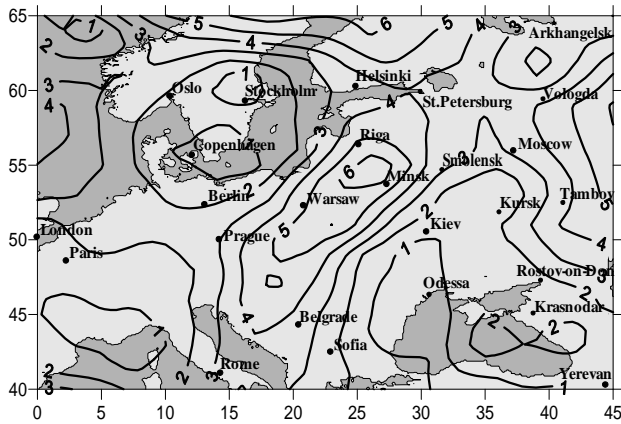
a)



b)



c)



-- wind ($|\vec{V}|$) top scale, - · - potential temperature (θ) middle scale,
 — turbulence coefficient (K) bottom scale.

1. Berkovich L, Tarnopolskiy A., Shnaydman V, (1997) Hydrodynamic model of the atmospheric and oceanic boundary layers. Russian Meteorology and Hydrology **7**, 40-52.

2. Shnaydman V. (2010) Improved numerical solution of three-dimensional turbulence closure equations Research Activity in Atmospheric and Oceanic Modeling #40, 4-13

Case study of a heavy rainfall event in Amami Island on 20 October 2010

Hiroshige TSUGUTI and Teruyuki KATO

Meteorological Research Institute / Japan Meteorological Agency, Tsukuba, Ibaraki, Japan
E-mail : htsuguti@mri-jma.go.jp

1. Introduction

On 20 October 2010, a heavy rainfall was observed in Amami Island, located in southern Japan. Figure 1 shows the horizontal distribution of daily accumulated Radar-Raingauge analyzed rainfall on 20 October 2010, which is estimated by meteorological Radar and calibrated using surface rain gauge observations. Areas with accumulated rainfall more than 200 mm are found widely over Amami Island, and the maximum value exceeds 800 mm. The daily accumulated rainfall of 622.0 mm was observed at the Naze meteorological observatory. This heavy rainfall caused serious disasters in Amami Island.

In this study, the characteristics of environmental fields and the development and maintenance mechanisms of precipitation systems inducing the heavy rainfall are examined from observations and numerical simulations results.

2. Supply of water vapor to Amami Island

Figure 2 shows the surface weather map at 09 LST (= UTC + 9 hours) on 20 October 2010. A stationary front is analyzed in an east-west direction in the vicinity of Amami Island. The center of Typhoon Megi with the minimum pressure of 945 hPa is located south of Taiwan. This synoptic pattern suggests the inflow of low-level humid air to the vicinity of Amami Island.

The 950 hPa-level water vapor flux field depicted from JMA mesoscale objective analysis data (MA) at 09 LST on 20 October 2010 are shown in Fig. 3. Water vapor flux larger than $300 \text{ g m}^{-2} \text{ s}^{-1}$ is found east of Amami Island. Air with the specific humidity larger than 16 g kg^{-1} was transported to Amami Island by strong easterly winds (not shown).

Vertical profiles of horizontal wind speed observed by the boundary layer radar at Naze are shown in Fig. 4. Easterly winds at a speed more than 16 m s^{-1} are predominant below a height of 2000 m, between 1000 LST and 1500 LST, when precipitation systems strongly developed over Amami Island. These results indicate that low-level humid air from the east contin-

uously flowed into Amami Island to develop and maintain the precipitation systems.

3. Terrain effect of Amami Island

The numerical model used in this study is the nonhydrostatic model (JMA-NHM, Saito et al., 2007) developed by the Japan Meteorological Agency (JMA). A double-moment bulk-type cloud microphysics scheme predicting the specific humidity of 6 water species (water vapor, cloud water, cloud ice, rain, snow, and graupel) and the number concentrations of 3 water species (cloud ice, snow and graupel) is employed. In this study, the JMA-NHM has a horizontal resolution of 1 km with 1000×800 grid points (1 km-NHM). The initial and boundary conditions of 1 km-NHM are produced from 3 hourly available MA with a horizontal resolution of 5 km. The initial time of 1 km-NHM is 1800 LST on 19 October 2010 and the forecast time is 30 hours (Fig. 5).

The 1 km-NHM (Fig. 6a) succeeds in producing regions of heavy rainfall, the location and distribution of which are similar to the observations (Fig. 1). Moreover, the simulated maximum daily rainfall agrees with the observations as well. To examine the terrain effect of Amami Island on the development and maintenance of the precipitation systems, a sensitivity experiment in which the topography of Amami Island is replaced with sea areas is performed. The sensitivity experiment result (Fig. 6b) is different from the control experiment (Fig. 6a). The daily accumulated rainfall near Amami Island is less than that in the control experiment. This result indicates that the terrain of Amami Island affected the development and maintenance of the precipitation systems inducing the heavy rainfall.

References

Saito, K., J. Ishida, K. Aranami, T. Hara, T. Segawa, M. Narita, and Y. Honda, 2007: Nonhydrostatic atmospheric models and operational development at JMA. *J. Meteor. Soc. Japan*, **85B**, 271-304.

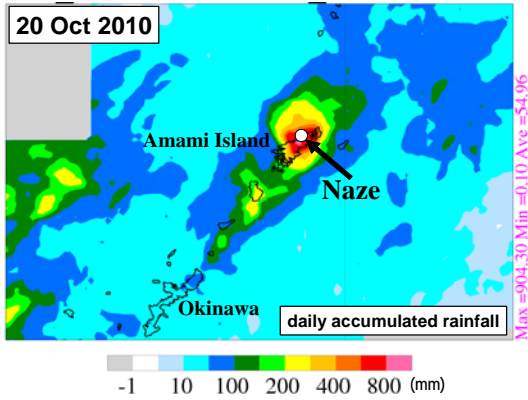


Fig. 1 Horizontal distribution of daily accumulated Radar-Raingauge analyzed rainfall on 20 October 2010.

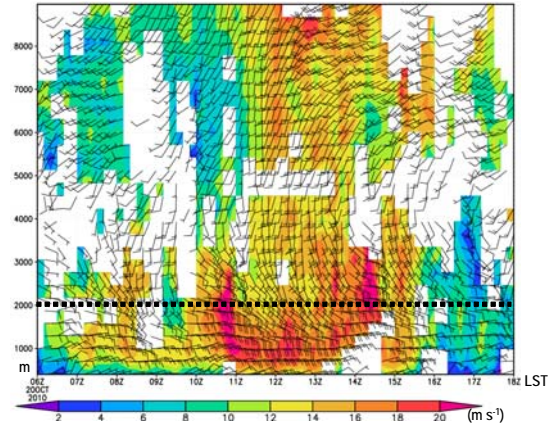


Fig. 4 Vertical profiles of horizontal wind speed (shaded) observed by the boundary layer radar at Naze from 0600 LST to 1800 LST on 20 October 2010. Half-barb means 5 m s^{-1} and Full-barb means 10 m s^{-1} . The black dashed line shows the height of 2000 m.

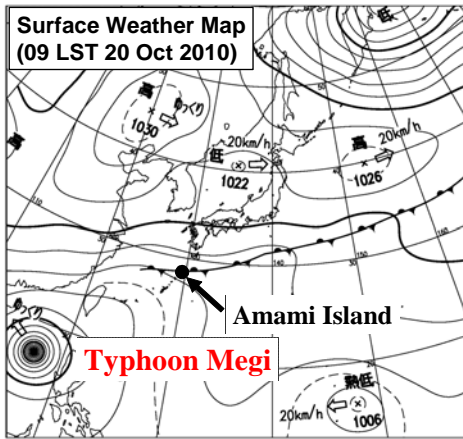


Fig. 2 Surface weather map at 09 LST on 20 October 2010.

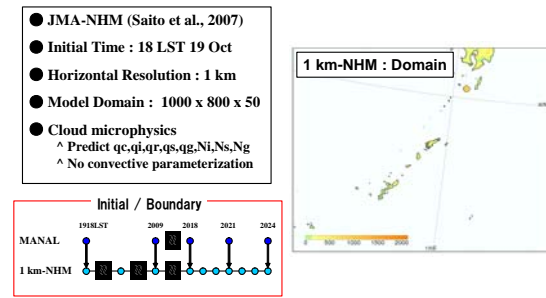


Fig. 5 Numerical experiment design and calculation domain of 1 km-NHM.

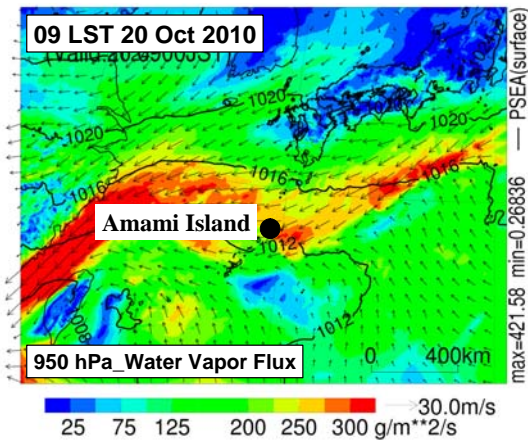


Fig. 3 950 hPa-level water vapor flux field and horizontal winds depicted from MA at 09 LST on 20 October 2010.

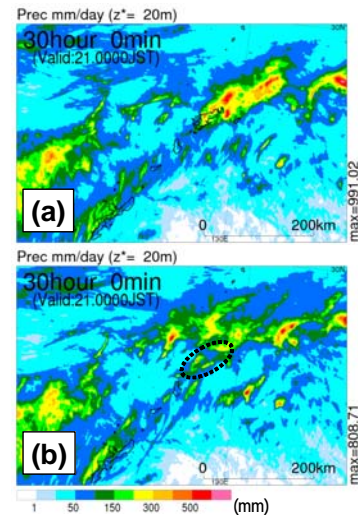


Fig. 6 Same as Fig. 1, but simulated by 1 km-NHM. (a) the control experiment and (b) the sensitivity experiment in which the topography of Amami Island is replaced with sea areas. The dashed circle in (b) shows the location of Amami Island.